Supporting Information

Oxygen substitution at unbonded S site for excellent wet-air stability and lithium compatibility of Br-rich Li-argyrodite solid-state electrolytes

Haiting Shi[a], Tong Xu[a], Daoxi Wang[a], Xianyan Wu[b*], Shuaitong Liang[c*], Yaohui Liang[d*], Hao Li[e], Zhiwei Xu[*a]

[a] State Key Laboratory of Separation Membranes and Membrane Processes, School of Textile Science and Engineering, Tiangong University, Tianjin 300387, China
[b] College of Materials and Textile Engineering, Nanotechnology Research Institute, Jiaxing University, Jiaxing 314001, China
[c] International Joint Laboratory of New Textile Materials and Textiles of Henan Province, Zhongyuan University of Technology, Zhengzhou 450007, China
[d] College of Electronic Information Engineering, Key Laboratory of Brain-like Neuromorphic Devices and Systems Hebei Province, Hebei University, Baoding, 071002, China
[e] Key Laboratory of Neutron Physics, Institute of Nuclear Physics and Chemistry, China Academy of Engineering Physics, Mianyang 621999, China

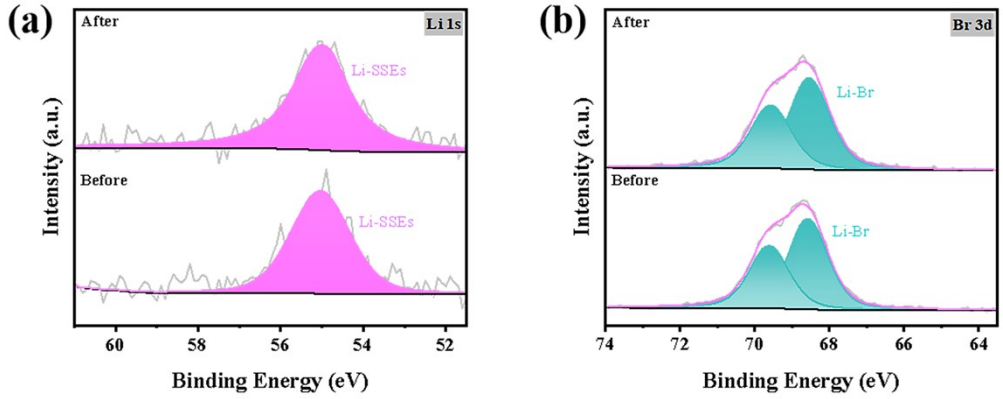

Fig. S1 XPS spectra of $Li_{5.6}PS_{4.6-x}O_xBr_{1.4}$ (x = 0, 0.15) SSEs before and after O-doping. a) Li 1s. b) Br 3d.

* Corresponding author. E-mail address: xywu@zjxu.edu.cn(Xianyan Wu); shuaitongliang@zut.edu.cn (Shuaitong Liang); liangyh@hbu.edu.cn(Yaohui Liang); xuzhiwei@tiangong.edu.cn(Zhiwei Xu)

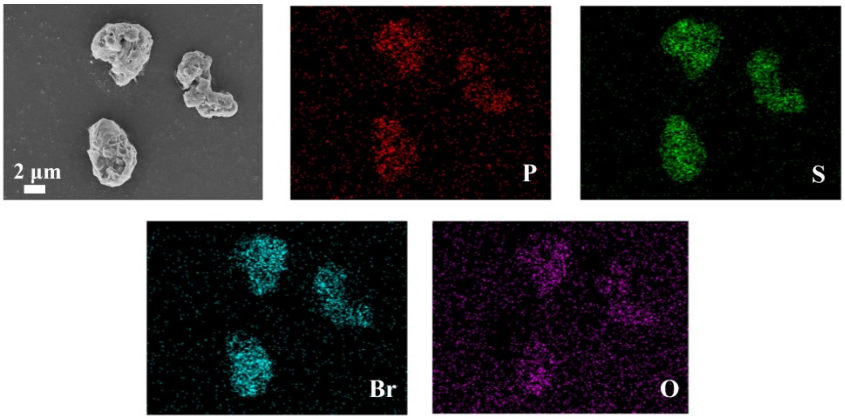

Fig. S2 SEM and EDS mapping of $Li_{5.6}PS_{4.6-x}O_xBr_{1.4}$ (x = 0.05) electrolyte.

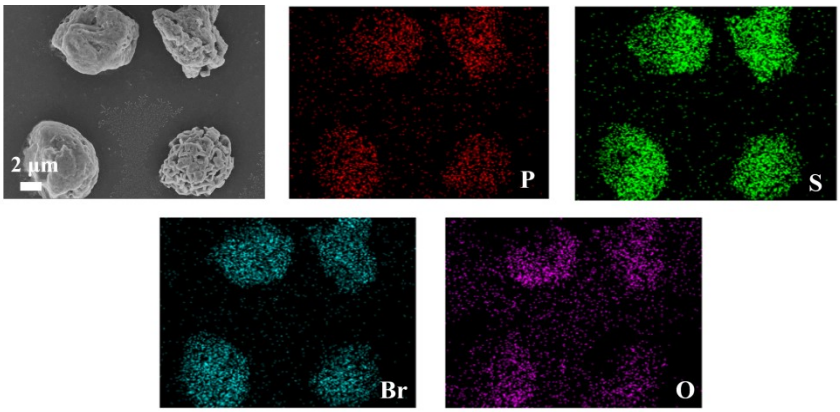

Fig. S3 SEM and EDS mapping of $Li_{5.6}PS_{4.6-x}O_xBr_{1.4}$ (x = 0.1) electrolyte.

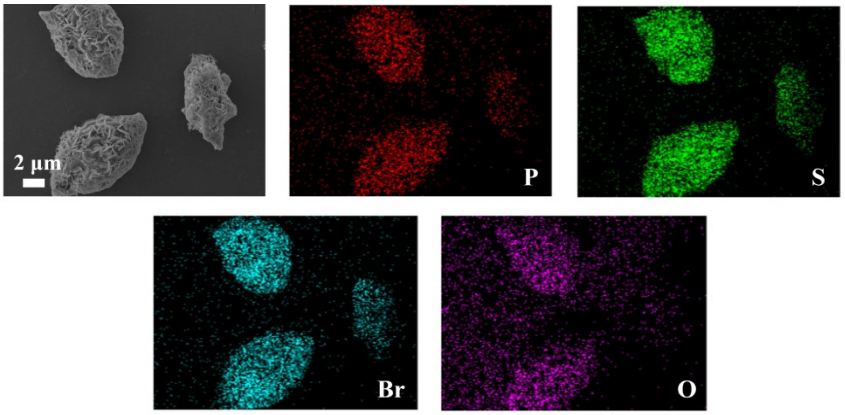

Fig. S4 SEM and EDS mapping of $Li_{5.6}PS_{4.6-x}O_xBr_{1.4}$ (x = 0.2) electrolyte.

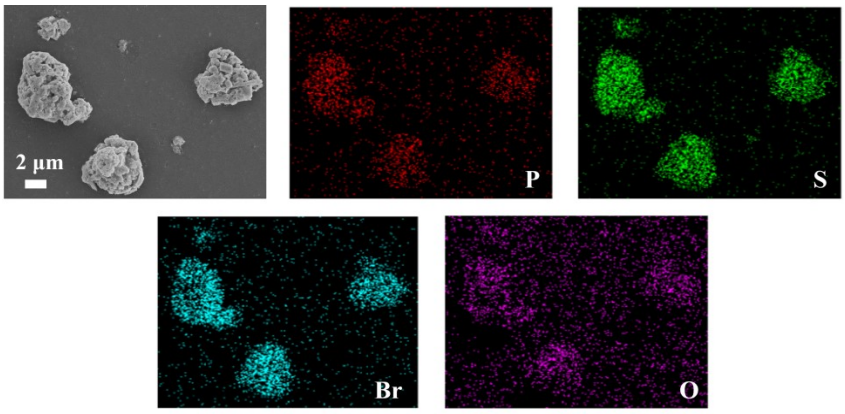

Fig. S5 SEM and EDS mapping of $Li_{5.6}PS_{4.6-x}O_xBr_{1.4}$ (x = 0.25) electrolyte.

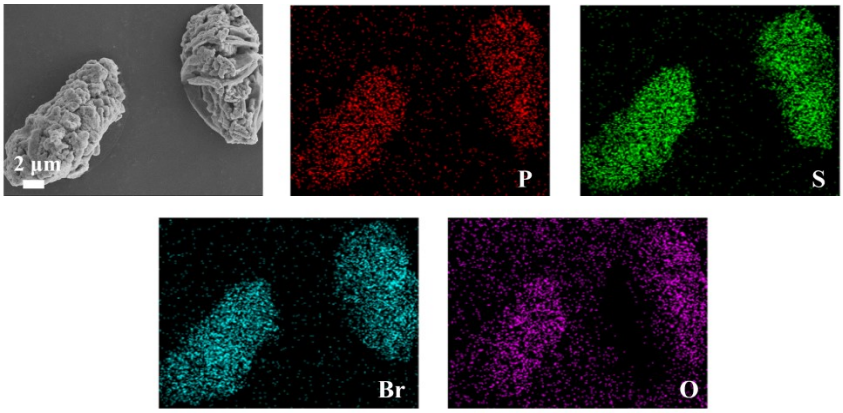

Fig. S6 SEM and EDS mapping of $Li_{5.6}PS_{4.6-x}O_xBr_{1.4}$ (x = 0.3) electrolyte.

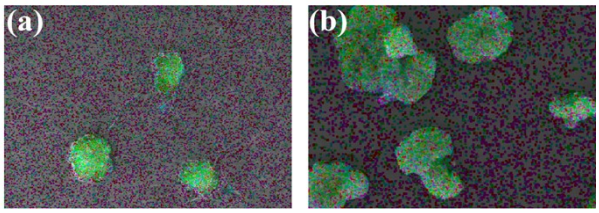

Fig. S7 EDS layered maps of (a) $Li_{5.6}PS_{4.6}Br_{1.4}$ and (b) $Li_{5.6}PS_{4.45}O_{0.15}Br_{1.4}$ electrolytes.

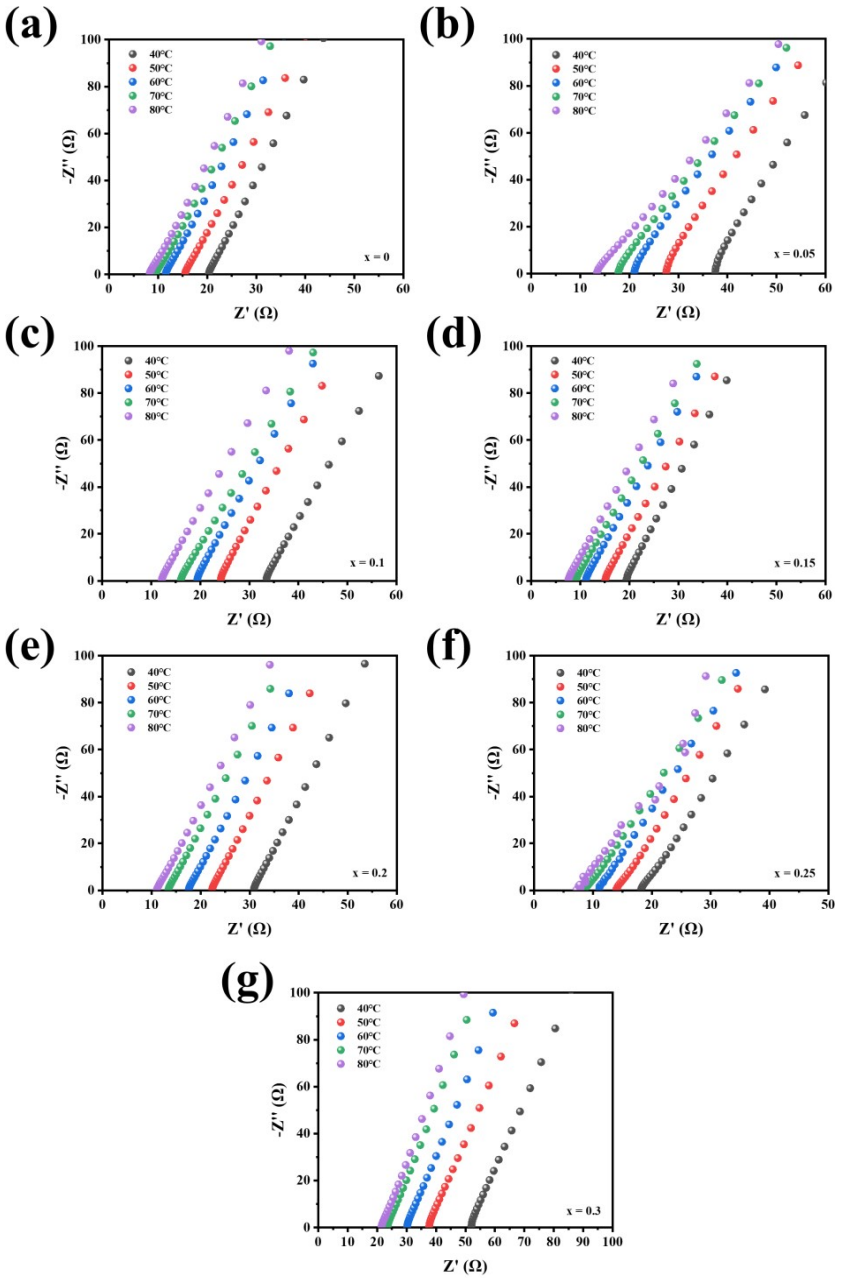

Fig. S8 Nyquist plots of $Li_{5.6}PS_{4.6-x}O_xBr_{1.4}$ electrolytes in different temperature ranges (40-80 °C), where (a) x = 0, (b) x = 0.05, (c) x = 0.1, (d) x = 0.15, (e) x = 0.2, (f) x = 0.25, (g) x = 0.3.

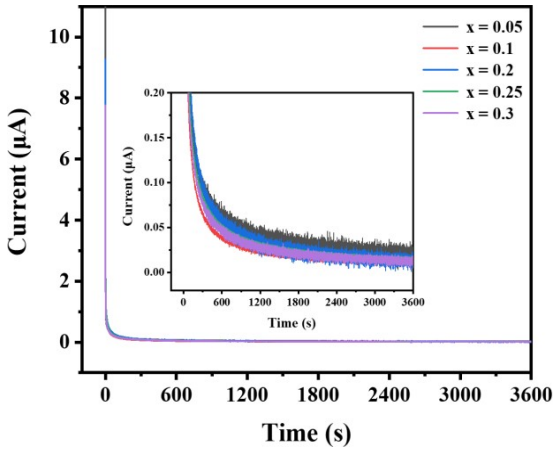

Fig. S9 DC polarization curves for $Li_{5.6}PS_{4.6-x}O_xBr_{1.4}$ (x = 0.05, 0.1, 0.2, 0.25, 0.3) electrolytes.

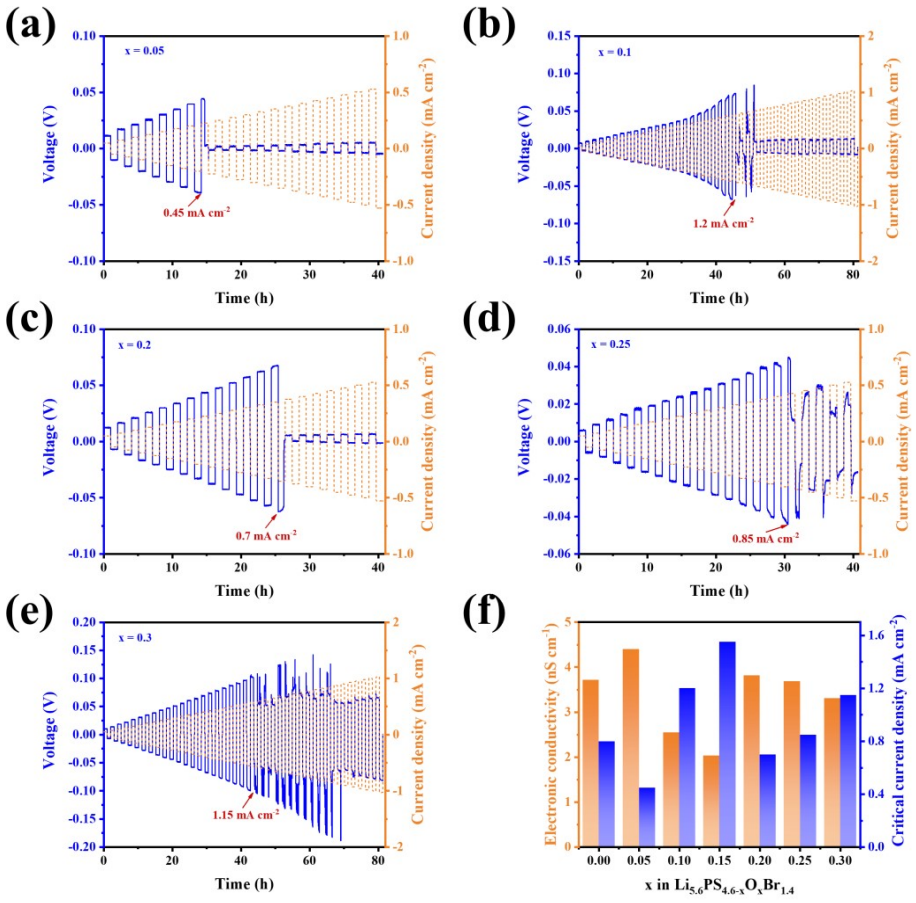

Fig. S10 Constant-current cycling of a Li symmetric cell using the $Li_{5.6}PS_{4.6-x}O_xBr_{1.4}$ electrolytes at room temperature with progressively increasing current density, where (a) x = 0.05, (b) x = 0.1, (c) x = 0.2, (d) x = 25, and (e) x = 0.3; (f) CCD and electronic conductivity as a function of different O substitution concentrations.

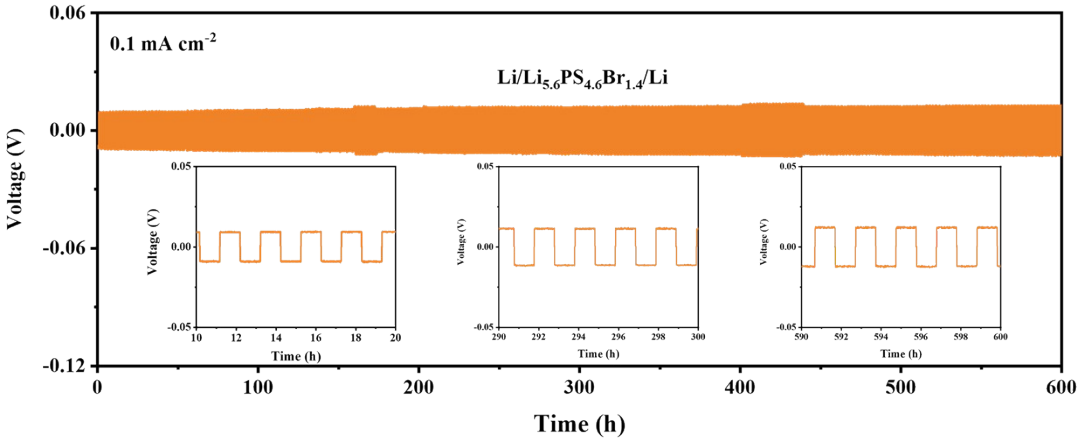

Fig. S11 Constant-current cycling at 0.1 mA cm^{-2}/0.1 mAh cm^{-2} of a Li symmetric cell using $Li_{5.6}PS_{4.6}Br_{1.4}$ electrolyte.

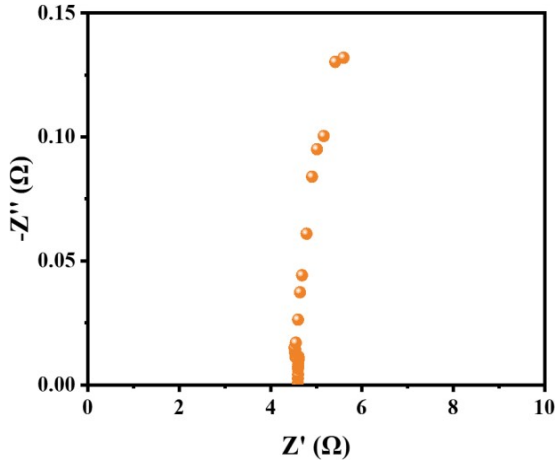

Fig. S12 Nyquist plots of Li/$Li_{5.6}PS_{4.6}Br_{1.4}$/Li symmetric cells after cycling at 0.5 mA cm^{-2} for 10 h at room temperature.

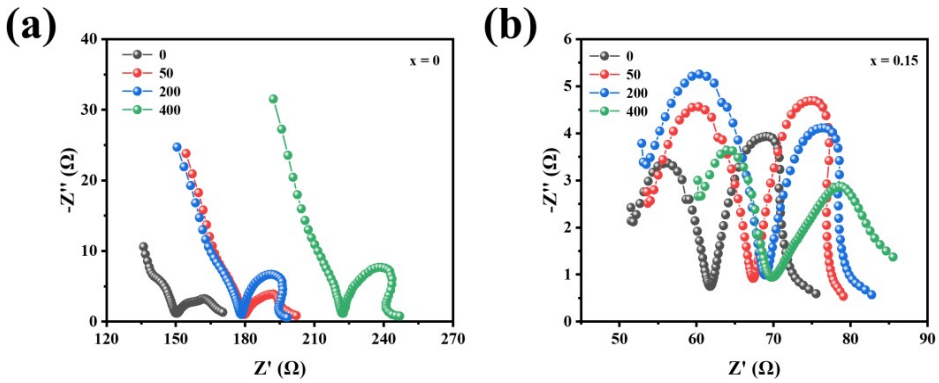

Fig. S13 Changes in impedance spectra of (a) Li/$Li_{5.6}PS_{4.6}Br_{1.4}$/Li and (b) Li/$Li_{5.6}PS_{4.45}O_{0.15}Br_{1.4}$/Li symmetric cells after different durations of lithium stripping/plating at 0.1 mA cm^{-2}.

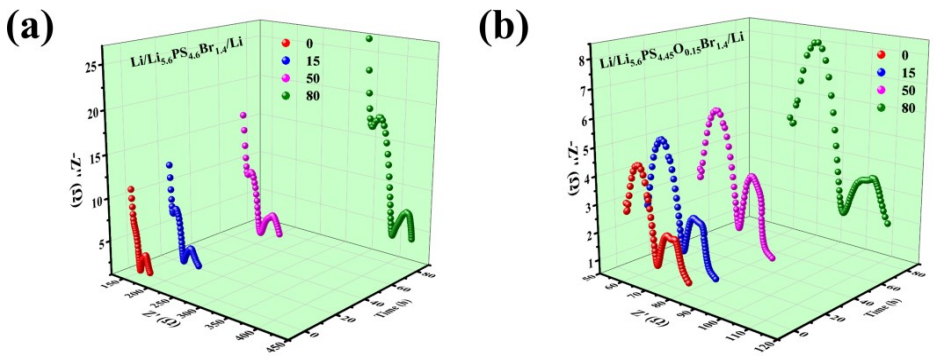

Fig. S14 Impedance spectra of Li symmetric cell consisting of (a) $Li_{5.6}PS_{4.6}Br_{1.4}$ and (b) $Li_{5.6}PS_{4.45}O_{0.15}Br_{1.4}$ electrolytes at room temperature with storage time.

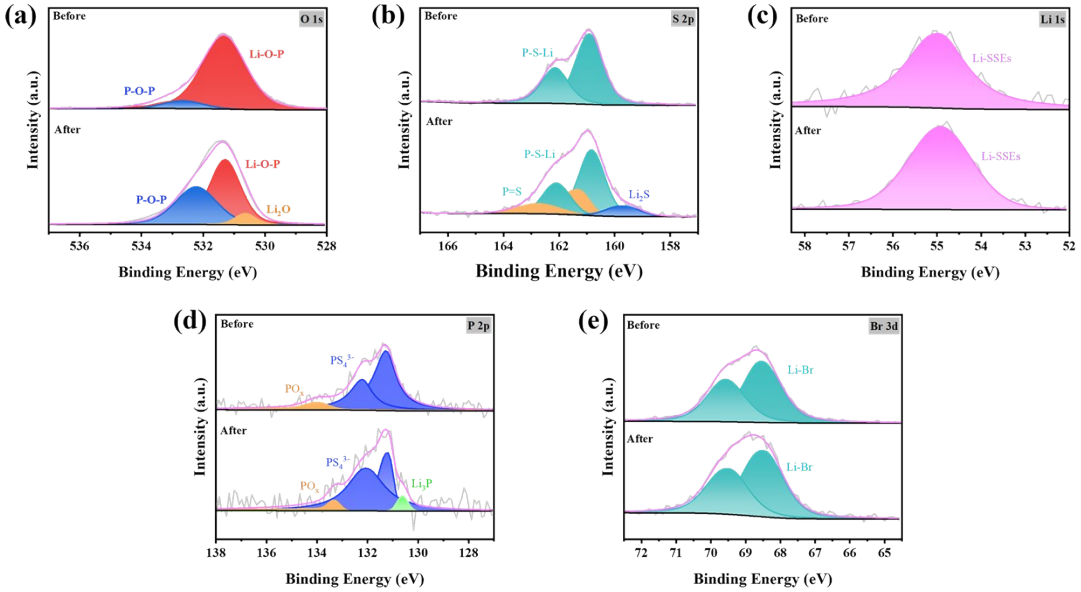

Fig. S15 XPS deconvolution spectra of Li/$Li_{5.6}PS_{4.45}O_{0.15}Br_{1.4}$ interface before and after cycling for 80 h at 0.2 mA cm^{-2}. a) O 1s. b) S 2p. c) Li 1s. d) P 2p. e) Br 3d.

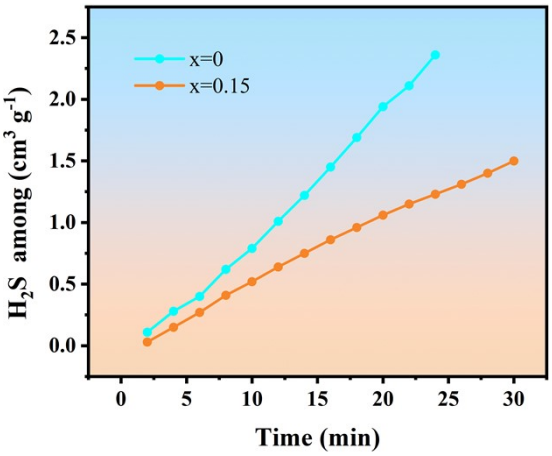

Fig. S16 H_2S content released from $Li_{5.6}PS_{4.6}Br_{1.4}$ and $Li_{5.6}PS_{4.45}O_{0.15}Br_{1.4}$ electrolytes after exposure to wet-air at 30% humidity for 30 min.

Table S1 Crystallographic data (atomic coordinates, occupancy, and Beq) of $Li_{5.6}PS_{4.6}Br_{1.4}$, obtained from Rietveld refinement of neutron diffraction data.

$Li_{5.6}PS_{4.6}Br_{1.4}$ structure from neutron diffraction data (space group F-43m); **λ_1 = 1.8838 Å;** **a = 9.978659 Å;** **Fit residuals (R_{wp}, R_{exp}, R_p): 4.008%, 4.108%, 3.110%;**						
Atom	**Wyckoff site**	**x**	**y**	**z**	**Occ.**	**Beq**
Li1 (T5)	48h	0.3164	0.0262	0.7045	0.18554	0.91907
Li2 (T2)	48h	0.2658	0.0495	0.6630	0.12510	0.86720
P1	4b	0.0000	0.0000	0.5000	1.00000	1.81500
S1	16e	0.1200	-0.1200	0.6027	1.00000	3.00000
S2	4d	0.2500	0.2500	0.7500	0.41332	2.72668
S3	4a	0.0000	0.0000	1.0000	0.0520	0.07156
Br1	4d	0.2500	0.2500	0.7500	0.58668	0.30339
Br2	4a	0.0000	0.0000	1.0000	0.95881	0.22855

Table S2 Crystallographic data (atomic coordinates, occupancy, and Beq) of $Li_{5.6}PS_{4.45}O_{0.15}Br_{1.4}$, obtained from Rietveld refinement of neutron diffraction data.

$Li_{5.6}PS_{4.45}O_{0.15}Br_{1.4}$ structure from neutron diffraction data (space group F-43m); **λ_1 = 1.8838 Å;** **a = 9.979071 Å;** **Fit residuals (R_{wp}, R_{exp}, R_p): 4.867%, 3.947%, 3.827%;**						
Atom	**Wyckoff site**	**x**	**y**	**z**	**Occ.**	**Beq**
Li1 (T5)	48h	0.2895	0.0217	0.67928	0.22239	1.49954
Li2 (T2)	48h	0.2580	0.0495	0.6635	0.14520	0.85430
P1	4b	0.0000	0.0000	0.5000	1.00000	1.86818
S1	16e	0.1200	-0.1200	0.59634	1.00000	0.29360
S2	4d	0.2500	0.2500	0.7500	0.20398	2.67166
S3	4a	0.0000	0.0000	1.0000	0.34382	0.00000
Br1	4d	0.2500	0.2500	0.7500	0.68167	2.67166
Br2	4a	0.0000	0.0000	1.0000	0.65618	0.00000
O1	4d	0.2500	0.2500	0.7500	0.11435	2.67166

Table S3 Table of elemental At % occupancy of $Li_{5.6}PS_{4.6-x}O_xBr_{1.4}$ ($0 \leq x \leq 0.3$) at different oxygen doping levels.

Distribution of total number of spectra							
Different oxygen doping (x)	**0**	**0.05**	**0.1**	**0.15**	**0.2**	**0.25**	**0.3**
O(At%)	**0.12**	**0.7**	**1.43**	**2.14**	**2.86**	**3.59**	**4.29**
S(At%)	**67**	**65**	**64.29**	**63.57**	**62.87**	**62.14**	**61.82**
P(At%)	**15**	**14.3**	**14.4**	**13.98**	**14.2**	**14.66**	**14.68**
Br(At%)	**17.88**	**20**	**19.88**	**20.31**	**20.07**	**19.61**	**19.21**
Total amount	**100**	**100**	**100**	**100**	**100**	**100**	**100**
O/S	**0.0067**	**0.0108**	**0.0222**	**0.0337**	**0.0454**	**0.0578**	**0.0694**

Table S4 Summary of the sulfide electrolyte-based Li-Li symmetric cell performance.

Name of SSEs	CCD (mA cm^{-2})	Plating Current Density (mA cm^{-2})	Cut-off Capacity (mAh cm^{-2})	Cycling Time (h)	Test Temperature (℃)	Reference
$Li_{5.6}PS_{4.45}O_{0.15}Br_{1.4}$	**1.55**	**0.1**	**0.1**	**600**	**25**	**This work**
		0.5	**0.5**	**～400**	**25**	
$Li_{5.5}PS_{4.425}O_{0.075}Cl_{1.5}$	-	0.4	0.2	150	25	[1]
$Li_{6.03}P_{0.97}Se_{0.03}S_5Cl$	0.6	0.1	-	185	25	[2]
$Li_{6.04}P_{0.98}Bi_{0.02}S_{4.97}O_{0.03}Cl$	1.1	0.1	0.1	600	25	[3]
		1	1	200	25	
$Li_{5.6}PS_{4.6}Cl_{1.0}Br_{0.4}$	0.35	0.2	-	500	25	[4]
$Li_{5.95}Zn_{0.025}PS_{4.975}O_{0.025}Cl$	0.55	0.4	-	100	25	[5]
$Li_{5.7}Zn_{0.15}PS_{4.85}O_{0.15}Br$	0.78	0.78	0.39	140	25	[6]
LPSScO(0.15)-22.5LiS	0.6	0.2	-	300	25	[7]
		0.3	-	200	25	
$Li_7P_{2.88}Nb_{0.12}S_{10.7}O_{0.3}$	1.16	0.2	0.2	300	25	[8]
$Li_{6.125}P_{0.875}Sn_{0.125}S_5Br$	0.8	0.1	0.1	400	25	[9]
$Li_{6.3}P_{0.7}Sn_{0.3}S_{4.4}O_{0.6}I$	0.75	0.2	0.1	180	25	[10]
$Li_{5.6}PS_{4.6}Cl_{1.3}I_{0.1}$	1.74	0.1		500	24	[11]
$Li_{6.16}P_{0.92}In_{0.08}S_{4.88}O_{0.12}Cl$	1.4	0.1	0.1	3000	25	[12]
		0.5	0.5	500		
		1	1	400		

References

1. L. F. Peng, S. Q. Chen, C. Yu, C. C. Wei, C. Liao, Z. K. Wu, H. L. Wang, S. J. Cheng and J. Xie, *ACS Appl. Mater. Interfaces.*, 2022, **14**, 4179-4185.
2. H. M. Kim, Y. Subramanian and K. S. Ryu, *Electrochim. Acta*, 2023, **442**, 141869.
3. H. Liu, Q. S. Zhu, C. Wang, G. X. Wang, Y. H. Liang, D. B. Li, L. Gao and L. Z. Fan, *Adv. Funct. Mater.*, 2022, **32**, 2203858.
4. Y. Subramanian, R. Rajagopal and K. S. Ryu, *J. Power Sources*, 2022, **520**, 230849.
5. G. J. Jang, R. Rajagopal, S. Kang and K. S. Ryu, *J. Alloys Compd.*, 2023, **957**, 107273.
6. T. Chen, L. Zhang, Z. X. Zhang, P. Li, H. Q. Wang, C. Yu, X. L. Yan, L. M. Wang and B. Xu, *ACS Appl. Mater. Interfaces.*, 2019, **11**, 40808-40816.
7. Y. Subramanian, R. Rajagopal, S. Kang, Y. J. Jung and K. S. Ryu, *J. Energy Storage*, 2023, **68**, 107715.
8. Z. Jiang, T. B. Liang, Y. Liu, S. Z. Zhang, Z. X. Li, D. H. Wang, X. L. Wang, X. H. Xia, C. D. Gu and J. P. Tu, *ACS Appl. Mater. Interfaces.*, 2020, **12**, 54662-54670.
9. S. H. Choi, W. J. Kim, B. H. Lee, S. C. Kim, J. G. Kang and D. W. Kim, *J. Mater. Chem. A*, 2023, **11**, 14690-14704.
10. T. Chen, D. W. Zeng, L. Zhang, M. Yang, D. W. Song, X. L. Yan and C. Yu, *J. Energy Chem.*, 2021, **59**, 530-537.
11. H. Yan, R. F. Song, R. A. Xu, S. L. Li, Q. Q. Lin, X. L. Yan, Z. Y. Wang, C. Yu and L. Zhang, *J. Energy Chem.*, 2023, **86**, 499-509.
12. C. D. Wang, J. M. Hao, J. Wu, H. F. Shi, L. B. Fan, J. S. Wang, Z. K. Wang, Z. Wang, L. Yang, Y. Gao, X. Q. Yan and Y. S. Gu, *Adv. Funct. Mater.*, 2024, **34**, 2313308.